Theoretical Population Biology **62**, 63–80 (2002)
doi:10.1006/tpbi.2002.1581, available online at http://www.idealibrary.com on IDEAL®

TPB

Population-Level Consequences of Antipredator Behavior: A Metaphysiological Model Based on the Functional Ecology of the Leaf-Eared Mouse

Rodrigo Ramos-Jiliberto

Centro de Estudios Avanzados en Ecología & Biodiversidad, Departamento de Ecología, P. Universidad Católica de Chile, Casilla 114-D, Santiago, Chile
E-mail: rramos@bio.puc.cl

Eduardo González-Olivares

Instituto de Matemáticas, Facultad de Ciencias Básicas y Matemáticas, Universidad Católica de Valparaíso, Chile

and

Francisco Bozinovic

Centro de Estudios Avanzados en Ecología & Biodiversidad, Departamento de Ecología, P. Universidad Católica de Chile, Casilla 114-D, Santiago, Chile

Received October 2, 2001

We present a predator–prey metaphysiological model, based on the available behavioral and physiological information of the sigmodontine rodent *Phyllotis darwini*. The model is focused on the population-level consequences of the antipredator behavior, performed by the rodent population, which is assumed to be an inducible response of predation avoidance. The decrease in vulnerability is explicitly considered to have two associated costs: a decreasing foraging success and an increasing metabolic loss. The model analysis was carried out on a reduced form of the system by means of numerical and analytical tools. We evaluated the stability properties of equilibrium points in the phase plane, and carried out bifurcation analyses of rodent equilibrium density under varying conditions of three relevant parameters. The bifurcation parameters chosen represent predator avoidance effectiveness (A), foraging cost of antipredator behavior (C_1'), and activity-metabolism cost (C_4'). Our analysis suggests that the trade-offs involved in antipredator behavior plays a fundamental role in the stability properties of the system. Under conditions of high foraging cost, stability decreases as antipredator effectiveness increases. Under the complementary scenario (not considering the highest foraging costs), the equilibria are either stable when both costs are low, or unstable when both costs are higher, independent of antipredator effectiveness. No evidence of stabilizing effects of antipredator behavior was found.

Key Words: **predation; refuge; stability; bifurcation.**

1. INTRODUCTION

Since the pioneer works of Alfred Lotka and Vito Volterra, theoretical models of food web dynamics have developed considerably by incorporating essential biological details, which in turn may have dramatic effects on the modeled population behavior. In the domain of predator–prey models, one of such advances was the explicit incorporation of negative feedback (self-limitation). This approach attempts to account for

0040-5809/02 $35.00

intra-specific competition among individuals belonging to the population of prey, or both prey and predators (Leslie, 1948). Dampened oscillations converging to a community steady state was a major population-level novelty gained with the incorporation of self-limited growth (see Berryman, 1992). Other paradigmatic progress was achieved with the inclusion of features related to the foraging behavior of predators, the so-called functional responses or extraction functions. In the original Lotka–Volterra predation model, predators are assumed to be insatiable. However, assuming individual consumption to be an asymptotic function of prey density (Holling, 1959) results in models with new static and dynamic properties, including the occurrence of limit cycles (Murdoch and Oaten, 1975; Harrison 1979).

Much less theoretical work has been done with regard to the behavior of prey and its consequences on the whole system (Sih, 1987a; Sih *et al.*, 1988). One of the most noticeable properties of prey is their capability to face predation by means of several physiological, morphological and behavioral strategies, which reduce the probability of being detected, captured, killed or ingested (Sih, 1987b).

A moderate number of theoretical works have dealt with the reduction of prey vulnerability in the context of predator–prey models, typically through the use of spatial refuges. These safe places are often assumed to protect either a fixed number of prey or a fixed proportion of prey (Maynard-Smith, 1974). The familiar conclusion that refuge use by the prey promotes stability (Maynard-Smith, 1974; Murdoch and Oaten, 1975; Harrison, 1979; see also McNair, 1986; Křivan, 1998) is now being considered with caution, since it works only for very simple models, and because empirical evidence of such an effect is scarce (McNair, 1986). Indeed, the occurrence of a constant number or a constant proportion of prey in refuge seems to be very unlikely in nature (Sih, 1987a).

Ruxton (1995) considered another striking feature of antipredator behavior, that is, an often reversible response to predation risk. The inducible character of the response precludes the existence of costs under decreasing predation; otherwise the trait is expected to be fixed (Harvell and Tollrian, 1999). The cost of predation avoidance is commonly assumed to decrease intrinsic growth rate (Sih, 1987a) through lowering birth rate or through increasing background (non-predation) mortality rate. From an individual point of view, decreased birth rate as a result of refuge use could be explained either through lowering foraging rate, increasing metabolic loss, decreasing reproductive effort, and/or decreasing mating success. On the other hand, an increased background mortality rate could be due to physiological stress derived from starvation, crowding, or sub-optimal physical conditions in the refuge.

There is an increasing concern about the topic of "inducible defenses" in ecology and evolution (see Tollrian and Harvell, 1999) and this phenomenon seems to be widely spread across taxa and ecosystems. Nevertheless, few theoretical papers have incorporated inducible antipredator responses as an essential ingredient in modeling trophic interactions. In this work, we focus on the behavior of refuge use by a rodent population, which is assumed to be an inducible mechanism of predation avoidance. We consider that a decrease in prey vulnerability (see Abrams and Walters, 1996) has the associated costs of decreasing foraging and of increasing metabolic loss.

To explicitly formulate the trade-offs in terms of functional relationships between prey vulnerability and biomass fluxes through foraging and metabolism, we used a metaphysiological approach to modeling population dynamics (Getz, 1991, 1993, 1994). The fundamentals of this approach are to model populations as a single meta-organism characterized by its biomass density, whose rate of change is governed by processes related to resource extraction and conversion, and whose rate of biomass loss depends on metabolic expenditure and predator outflow. We designed and analyzed a metaphysiological model of the sigmodontine rodent *Phyllotis darwini* considering what is known regarding the behavioral and physiological information of this species. Our main goal was to explore the population-level consequences of the predator-induced behavior of refuge use by the rodent population, and allowing for the occurrence of previously evidenced trade-offs.

1.1. Biological Background

The populations of the leaf-eared mouse *P. darwini* have been shown to be numerically dominant and largely irruptive among the small mammal assemblage of central-north Chile (Jimenez *et al.*, 1992; Jaksic, 1997). *P. darwini* uses open scrubs as typical habitat, it is an omnivore (feeding mainly on seeds and small herbs), reproduces between September and January, and has an average adult body mass of nearly 50 g (Meserve, 1981; Meserve and LeBoulengé, 1987; see also Jaksic, 1997). On the other hand, *P. darwini* seems to strongly interact with owl predators (Meserve *et al.*, 1996; Lima *et al.*, 2001).

Recently, the population dynamics and demography of *P. darwini* have been studied on the basis of time-series analyses of a 14-year long survey in a semiarid locality of central Chile. These studies indicate that the population in this area is endogenously regulated by direct and delayed density dependence (Lima and Jaksic, 1998a, b; Lima *et al.*, 1999a). The interaction between exogenous forcing variables such as precipitation and endogenous dynamics, has a significant effect on population dynamics (Lima and Jaksic, 1999b; Lima *et al.*, 1999a, b, 2001).

The functional ecology of *P. darwini* is relatively well known (Jaksic, 1997), specially with regard to the effects of dietary composition, body size, ambient temperature and behavior on the energetics of this rodent (Bozinovic *et al.*, 1988; Bozinovic and Rosenmann, 1989; Ebensperger, 1996; Bozinovic, 1997; Bozinovic and Novoa, 1997; Bozinovic *et al.*, 1997; Canals *et al.*, 1997). Behavioral studies on *P. darwini* have revealed the importance of predation risk on microhabitat choice and feeding mode (Simonetti, 1989; Vásquez, 1994, 1996).

1.2. Numerical Analyses

The analysis of the model was carried out on a reduced form of the equations (Appendix A). We used the software XPPAUT 4.0 (Ermentrout, 2000) to assess the stability properties of the equilibrium points in the phase plane, and to obtain bifurcation diagrams of the equilibrium density of the focal rodent, after selecting three parameters to vary.

2. THE MODEL

The basic equation behind the metaphysiological modeling considers that the biomass X of the rodent population changes as a function of the per capita (here referred as per unit-biomass) rate of gross growth G, the per capita metabolic expenditure M, and the per capita mortality rate D:

$$\frac{dX}{dt} = X[G - M - D]. \tag{1}$$

The time unit of the model is 1 day, and the biomass is expressed in grams. The physiological parameters are commonly reported in other units, therefore we converted them to grams by using 1 ml $O_2 = 0.202$ kJ for respiration processes (Pitts and Sissom, 1979) and 1 g of mouse = 6.281 kJ (Gorecki, 1965; Kaufman *et al.*, 1975).

2.1. Rate of Gross Growth

Rate of gross growth is described here as the conversion function ξ_C of food ingestion $I(X)$, weighted by the digestive efficiency ξ_A:

$$G(X) = I(X)\xi_A\xi_C. \tag{2}$$

For simplicity, ξ_C is held constant, but it would be used in a more complex expression instead. Regarding the ingestion function, we used a generalized Holling-type with self-interference among consumers (Getz, 1984),

$$G(X) = \frac{gR^{\lambda}}{\beta^{\lambda} + (\gamma X)^{\lambda} + R^{\lambda}}\,\xi_A\xi_C, \tag{3}$$

where parameter g is the maximal ingestion rate per unit-biomass when the resource density R tends to infinity, β is the half-saturation parameter, γ is the self-interference term, and the exponent λ determines the presence or absence of an inflexion point in the curve. Whenever $\lambda = 1$, the function is a Holling type-II with self-interference (attributed to Beddington, 1975; DeAngelis *et al.*, 1975), whereas the curve is a Holling type-III when $\lambda > 1$.

2.2. Metabolic Expenditure

The per unit-mass metabolic expenditure defined in Eq. (4) has two additive components: the resting metabolic rate (μ_R) and the activity metabolic rate (μ_A). Although it is possible to consider the specific dynamic action (metabolic loss due to digestive activity, Grodzinski and Wunder, 1975) as a third component, this loss was implicitly incorporated into the conversion costs for simplicity (Eq. (3)):

$$M = \mu_R + \mu_A \tag{4}$$

with

$$\mu_A = \omega(\mu_M - \mu_R). \tag{5}$$

In other words, the currency invested in activity metabolism (i.e., for locomotion, food searching, escape) is assumed to be a fraction ω of the metabolic scope (defined herein as $S\mu_M - \mu_R$). μ_M is the maximum metabolic capacity of an average individual, and μ_R represents the energy allocated to thermoregulation. Thus, physiological thermoregulation is incorporated as a first priority in the energy-allocation "decision", as widely accepted for small mammals (Wunder, 1978; see also Bozinovic and Merritt, 1991).

2.3. Antipredator Response

Field and experimental evidence (Simonetti, 1989; Vásquez, 1994, 1996) suggest that *P. darwini* reacts to predation risk by means of changing its microhabitat use so as to minimize exposure to predators (mainly owls). Therefore, we assumed that prey vulnerability decreases with increasing predator density, from unity to a level V_α, as an effect of prey's antipredator behavior, according to the following function:

$$V(P) = \frac{1 - V_\alpha}{1 + (P/P_u)^z} + V_\alpha. \tag{6}$$

Equation (6) allows us to model prey vulnerability as a decreasing function of predator biomass (P), and its shape being either hyperbolic ($z = 1$), sigmoid ($z > 1$) or constant ($z = 0$). The value of z (if more than 1) defines the abruptness of the curve, which should be large if an on/off response takes place; P_u indicates the critical region of P where the antipredator response is induced (Fig. 1).

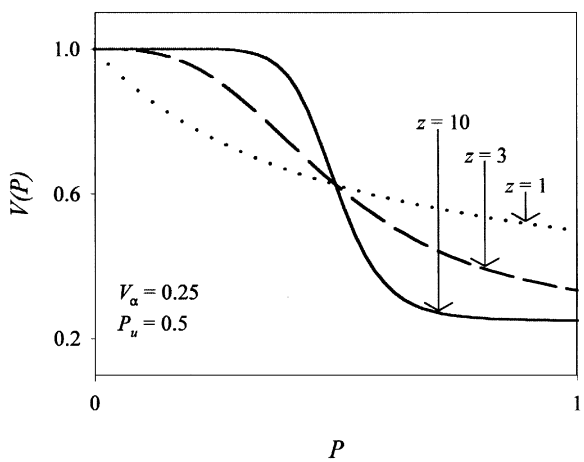

FIG. 1. Graphical representation of prey vulnerability (Eq. (6)) as a function of predator abundance. Three curves are shown for different values of parameter z. The inflexion point (with $z > 1$) is located at $P = P_u$. Parameter V_α sets the minimal vulnerability level when predator abundance is very high, thus being a measure of the effectiveness of the antipredator behavior.

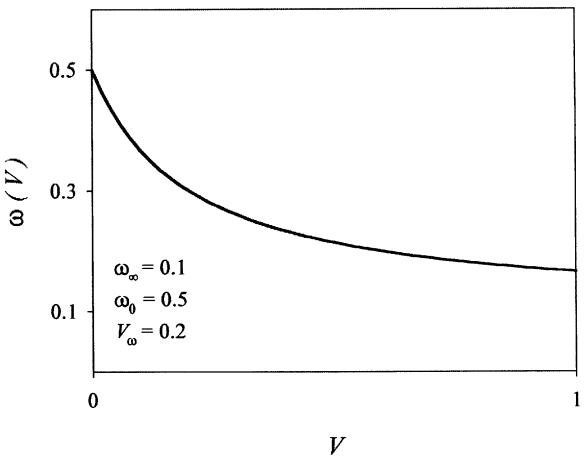

FIG. 2. Graphical representation of Eq. (7) relating allocation to activity metabolism and vulnerability. Since activity expenditure increases with antipredator behavior, it is a decreasing function of vulnerability, with maximum ω_0 and minimum ω_∞. The larger the differences between ω_0 and ω_∞ the higher is the metabolic cost, and vice versa. V_ω is a shape parameter that determines the slope of the curve when V tends to zero.

2.4. Trade-off between Vulnerability and Metabolic Loss

Changes in vulnerability as a response of predator density operate through modifications in habitat selection and foraging behavior, among others. Therefore, we considered an associated effect of vulnerability on activity metabolism. We formulated this trade-off as follows:

$$\omega(V) = \frac{V(\omega_\infty - \omega_0)}{V_\omega + V} + \omega_0. \tag{7}$$

Equation (7) represents the fraction of metabolic scope (see Eqs. (4) and (5)) allocated to activity. This fraction is made dependent on vulnerability, ω_∞ and ω_0 being the limits when V tends to infinity and zero, respectively. Parameter V_ω controls the shape of the curve (Fig. 2). Vásquez (1994, 1996) showed that the use of refuge by *P. darwini* increased its energy expenditure, which means that vulnerability to predators and activity metabolism are inversely related, or $\omega_\infty < \omega_0$.

2.5. Trade-off between Vulnerability and Foraging

Reducing vulnerability to predation involves the associated cost of decreasing food consumption (Vásquez, 1994, 1996). As before, the simplest saturating function to be used is

$$g(V) = \frac{V(g_\infty - g_0)}{V_g + V} + g_0, \tag{8}$$

where g_∞ and g_0 represent food consumption with unlimited food availability, under maximal and minimal

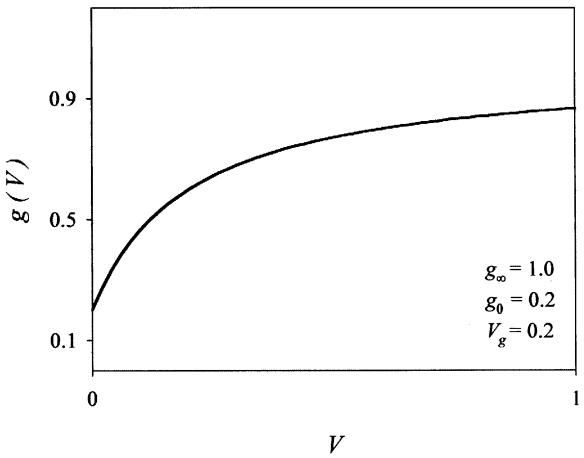

FIG. 3. Graphical representation of Eq. (8) relating food consumption (under unlimited food availability) to vulnerability. Lowering vulnerability decreases consumption. Minimum and maximum values are given by g_0 and g_∞, respectively. The larger the differences between g_∞ and g_0 the higher is the foraging cost, and vice versa. V_g is a shape parameter that determines the slope of the curve when V tends to zero.

vulnerability, respectively. Parameter V_g controls the shape of the hyperbolic function (Fig. 3).

2.6. Mortality Function

We used the same extraction function for both predators and prey, that is, a generalized Holling-type function with self-interference. Prey density is weighted by its vulnerability to account for the primary effect of antipredator behavior, which is to reduce predation loss. Thus, the biomass of prey eaten is given by

$$XD(X,P) = P\frac{\phi(VX)^{\Lambda}}{(VX)^{\Lambda} + \tau^{\Lambda} + (\Gamma P)^{\Lambda}}, \tag{9}$$

where ϕ is the limit when prey biomass tends to infinity, τ is the half-saturation parameter, and Γ is the self-interference term. The value of Λ defines the curve as being type II ($\Lambda = 1$) or type III ($\Lambda > 1$). By substituting Eq. (6) into (9), we obtain the complete expression for the mortality function:

$$D(X,P) = \frac{P\phi}{X}\left(1 + [\tau^{\Lambda} + (\Gamma P)^{\Lambda}] \times \left[\frac{P_u^z + P^z}{X(P_u^z + P^z V_\alpha)}\right]^{\Lambda}\right)^{-1}. \tag{10}$$

Likewise, by using Eqs. (3), (6) and (8) we obtain

$$G(X,P) = \frac{R^\lambda \xi_A \xi_C}{\beta^\lambda + (\gamma X)^\lambda + R^\lambda} \times \left[\frac{(g_\infty - g_0)(P_u^z + P^z V_\alpha)}{P_u^z(V_g + 1) + P^z(V_g + V_\alpha)} + g_0\right] \tag{11}$$

and if we consider Eqs. (4)–(7) we obtain

$$M(P) = \mu_R + \left[\frac{(\omega_\infty - \omega_0)(P_u^z + P^z V_\alpha)}{P_u^z(V_\omega + 1) + P^z(V_\omega + V_\alpha)} + \omega_0\right] \times (\mu_M - \mu_R). \tag{12}$$

2.7. Equation of Predators

Since we were not interested in the physiological variables of predators, we used a very simple equation for their dynamics. We assumed the population growth rate of predators to depend on prey extraction $H(X,P)$. This principle of biomass conversion is widely accepted in population models (Ginzburg, 1998).

$$\frac{dP}{dt} = f(H(X,P))P, \tag{13}$$

where $H(X,P)$ represents prey mortality per unit of predator biomass, and it is defined according to Eq. (9) as

$$H(X,P) = \frac{X}{P}D(X,P). \tag{14}$$

The non-linear conversion function used here (Getz, 1991) was

$$f(H(X,P)) = \rho\left[1 - \frac{\kappa}{H(X,P)}\right], \tag{15}$$

where ρ represents the upper limit of conversion rate of food extracted to growth, and κ the level of food extraction that allows population maintenance. Finally, the predator dynamics was expressed as

$$\frac{dP}{dt} = P\rho\left[1 - \frac{\kappa P}{XD(X,P)}\right]. \tag{16}$$

3. RESULTS AND DISCUSSION

The resulting model (Eqs. (10), (11) and (12) into (1) and (16), see also Tables I and II for a summary of the model components) was reparameterized. New state variables were defined as $p = P/P_u$ and $x = \gamma X/N^{1/\lambda}$, where $N = \beta^\lambda + R^\lambda$, and the equations recasted in the equivalent 14-parameter form (see Appendix A for

TABLE I

Variables and Functions of the Model

Symbol	Short definition	Argument	Units
	(I) *Variables*		
t	Time		d
X	Population size of prey		g
P	Population size of predator		g
	(II) *Functions*		
G	Per capita gross population growth rate	$g(V(P)), X$	d^{-1}
M	Per capita metabolic loss	$A(\omega(V(P)))$	d^{-1}
D	Per capita death rate	$P, X, V(P)$	d^{-1}
g	Maximal ingestion rate of prey	$V(P)$	d^{-1}
μ_A	Activity expenditure	$\omega(V(P))$	d^{-1}
V	Vulnerability to predation	P	dim. less
ω	Fraction of S allocated to activity metabolism	$V(P)$	dim. less.

details)

$$\frac{dx}{d\mathrm{T}} = x \times \left[\begin{array}{l} \left(\dfrac{A+p^z}{B_1+p^z}+C_1\right)\dfrac{1}{1+x^\lambda} - C_5\left(\dfrac{A+p^z}{B_2+p^z}+C_4\right) \\ -\dfrac{C_7 p}{x}\left[1+C_6\left(\dfrac{1+p^z}{x(A+p^z)}\right)^{\Lambda}(K_2+p^{\Lambda})\right]^{-1} \end{array} \right], \tag{17a}$$

$$\frac{dp}{d\mathrm{T}} = pC_9\left[1-K_5\left(\frac{1+p^z}{x(A+p^z)}\right)^{\Lambda}(K_2+p^{\Lambda})\right]. \tag{17b}$$

The points $(x, p) = (0, 0)$ and $(x_0, 0)$, where

$$x_0 = \left(\frac{A/B_1 + C_1}{C_5(A/B_2 + C_4)} - 1\right)^{1/\lambda} \tag{18}$$

can be shown to be equilibrium solutions to Eq. (17a,b).

There were also non-zero equilibrium points in the first quadrant which satisfy the transcendental equations:

$$1 - K_5\left(\frac{1+p^z}{x(A+p^z)}\right)^{\Lambda}(K_2+p^{\Lambda}) = 0 \tag{19}$$

and

$$\left(\frac{A+p^z}{B_1+p^z}+C_1\right)\frac{x}{1+x^\lambda} - C_5\left(\frac{A+p^z}{B_2+p^z}+C_4\right) - \frac{\phi C_7 p}{\kappa} = 0, \tag{20}$$

that is,

$$x = \left(\frac{1+p^z}{A+p^z}\right)[K_5(K_2+p^{\Lambda})]^{1/\Lambda}, \tag{21}$$

$$\frac{x}{1+x^\lambda} = \left(C_5\left(\frac{A+p^z}{B_2+p^z}+C_4\right) + \frac{\phi C_7 p}{\kappa}\right)\left(\frac{A+p^z}{B_1+p^z}+C_1\right)^{-1}. \tag{22}$$

For analysis, three parameters were selected according to their ecological relevance while all the others were assumed to be fixed. The selected parameters were

$$A = V_\alpha^{-1},$$

$$C_1 = \frac{g_0}{g_\infty - g_0}\frac{V_g + V_\alpha}{V_\alpha} \quad \text{and}$$

$$C_4 = \frac{V_\omega + V_\alpha}{V_\alpha(\omega_\infty - \omega_0)}\left(\frac{\mu_R}{\mu_M - \mu_R} + \omega_0\right).$$

Parameter A is interpreted as representing predator avoidance effectiveness, since lower values of V_α mean lower vulnerability to predation under high predator density. Parameter C_1 represents foraging effectiveness under reduced vulnerability, since large values of g_0 indicate that foraging remains closer to the maximum, under a fixed availability of resources. On the other hand, the absolute value of C_4 (which takes negative values) is directly related to resting metabolic rate (μ_R) of the animals, and inversely related to activity savings under reduced vulnerability. Thus, the greater the foraging and activity costs, the lower is the value of C_1 and the greater that of C_4, respectively. In order to better interpret the results, we rescaled C_1 and C_4 to

TABLE II

Parameters of the Model

Symbol	Short definition	Values	Ref	Units
R	Food availability	5×10^4–3×10^5	5	g
β	Half-saturation parameter of prey	> 0	0	g
λ	Functional response exponent of prey	$\geqslant 1$	0	dim.less
ξ_A	Digestive efficiency	0.6	4	dim.less
ξ_C	Conversion efficiency	0–1	0	dim.less
γ	Self-interference coefficient of prey	$\geqslant 0$	0	dim.less
μ_R	Specific resting metabolic rate	0.098–0.53	1	d^{-1}
μ_M	Specific maximal metabolic rate	> 0.53	2,3	d^{-1}
V_α	Vulnerability of prey under high predator density	0–1	0	dim.less
P_u	Predator density threshold for change in prey vulnerability	> 0	0	g
z	Abruptness of the vulnerability response to predation risk	$\geqslant 0$	0	dim.less
ω_0	Fraction of S allocated to activity metabolism under high predation risk	0–1	0	dim.less
ω_∞	Fraction of S allocated to activity metabolism under no predation risk	0–1	0	dim.less
V_ω	Shape controller of ω in response to V	$V_\alpha - 1$	0	dim.less
g_0	Food-satiation level with high predation risk	$0 - g_\infty$	0	d^{-1}
g_∞	Food-satiation level with no predation risk	0.1–0.22	4	d^{-1}
V_g	Shape controller of g in response to V	$V_\alpha - 1$	0	d^{-1}
ϕ	Maximal ingestion rate of predators	0.14–0.21	5	d^{-1}
τ	Half-saturation parameter of predators	> 0	0	g
Λ	Functional response exponent of predators	1–2	0	dim.less
Γ	Self-interference coefficient of predators	$\geqslant 0$	0	dim.less
ρ	Maximal per capita growth rate of predators	0.0035–0.0045	5	d^{-1}
κ	Per capita killing rate of prey needed for population maintenance of predators	0.05–0.1	5	d^{-1}

Note. All processes scaled to 1 ha. Data sources (Ref) as follows: (0) derived from model's assumptions and constraints; (1) Bozinovic and Rosenmann (1988); (2) Bozinovic *et al*. (1988); (3) Bozinovic and Rosenmann (1989); (4) Bozinovic and Nespolo (1997); (5) Own data.

$C_1' = 1 - C_1/30$ and $C_4' = 1 + C_4/10$, respectively. In this way, foraging cost and metabolic cost of activity will be shown as positive numbers and larger values will indicate larger costs. All other properties of the system that could alter the value of parameters are assumed to be constant.

Stability of the equilibria was explored using numerical analyses, where the values of the three parameters A, C_1' and C_4' were made to vary within plausible ranges by considering the approximations shown in Table II. Likewise, the fixed values used for the other parameters are shown in Table III.

The stability analyses are graphically summarized in Fig. 4. Three types of non-negative equilibria were found in the system: stable points, saddle points, and unstable points surrounded by at least one limit cycle, as will be shown below. Saddle points were associated to high values of C_1', that is to say, when foraging cost of predator avoidance is the highest. Under most parameter values, the equilibria are either stable or unstable. Stable points occur along with low values of C_4' (low cost of metabolic activity) for almost any combination of A and C_1', except at high values of A and C_1' (upper right corner of graphs) where unstable points appeared. For higher values of C_4' (from 0.68 up), an unstable band

TABLE III

New Parameters of the Reparameterized Model, with the Values Used for Numerical Analyses

Parameter	Value
λ	1.000
Λ	2.000
A	4.000
B_1	2.000
B_2	20.000
C_1	5.000
C_4	−3.000
C_5	−1.000
C_6	0.001
C_7	0.910
C_9	0.118
K_2	100.000
K_5	0.009
z	10.000

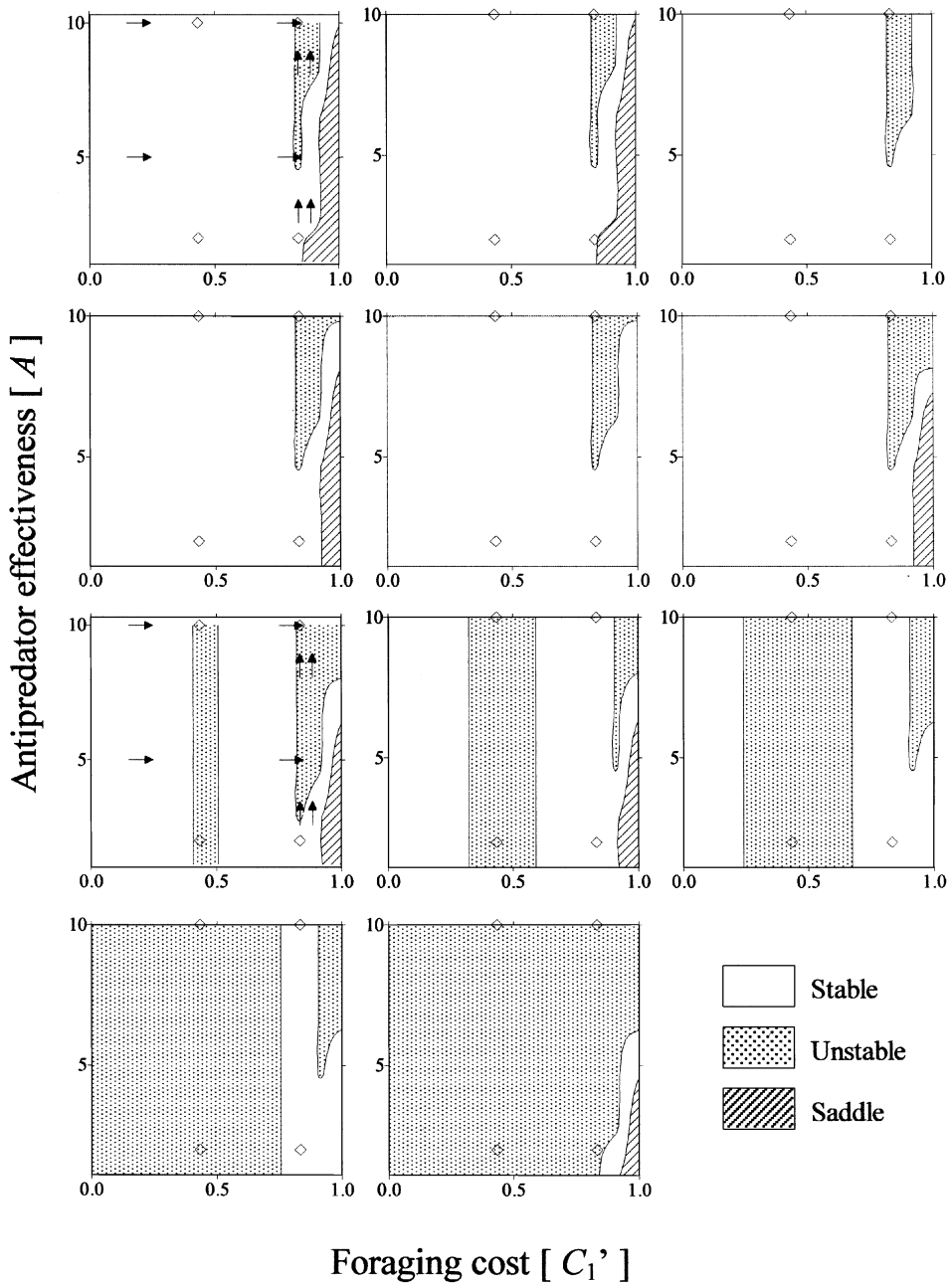

FIG. 4. Stability diagrams for the parameter space of antipredator effectiveness (parameter A, ordinate) and foraging cost (C_1', abscissa). The sequence of graphs resulted from the following values of metabolic cost (C_4') from upper left to lower right: 0.50, 0.53, 0.56, 0.59, 0.62, 0.65, 0.68, 0.71, 0.74, 0.77, 0.80. The sections crossed by arrows and diamonds were chosen for subsequent bifurcation analyses.

is found, which covers the entire range of A and an increasing fraction of the C_1' range as C_4' increases. Once C_4' reaches the maximum tested value (0.80), the whole parameter space formed by A and C_1' exhibits instability of the equilibrium point with the exception of the lower right corner (low A and high C_1').

A more detailed inspection was carried out on a subset of the parameter space by means of bifurcation analysis. Bifurcation diagrams taking A as the control parameter (also called bifurcation parameter) are shown in Fig. 5. The diagonal line of positive slope represents positive equilibrium density for rodents but zero for

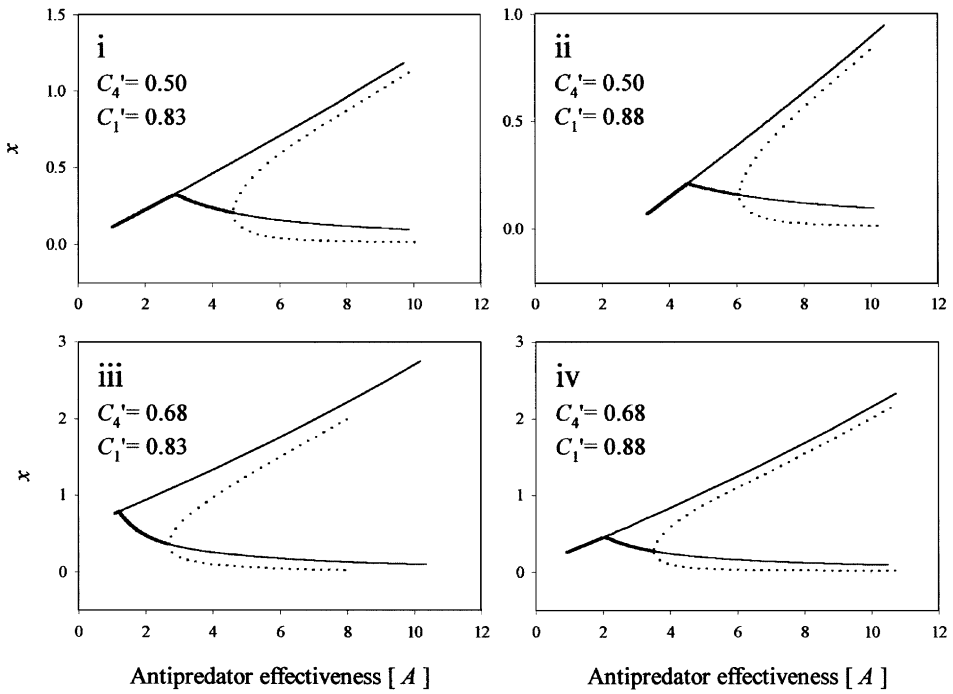

FIG. 5. Bifurcation diagrams when antipredator effectiveness is the control parameter. The values of C_1' and C_4' are shown inside the graphs (vertical arrows in Fig. 4): (thick line) stable fixed point; (thin continuous line) unstable fixed point; (dotted lines) maximum and minimum of stable orbits.

predators. This point is stable only at low values of A, and it is a saddle point for most values of the control parameter. The other equilibrium points shown in the graphs are positive for both prey and predator populations; as shown in Fig. 4, such equilibria were stable at low values and unstable at higher values of A. The rodent population acquired the maximum stable equilibrium density at the bifurcation point that separated the zero-predator equilibrium from the non-zero one. Accordingly, when the effectiveness of the rodent antipredator response is poor or null, the rodents reach a stable population density but their biomass increase is too low to maintain the predator population. If prey increase their antipredator effectiveness, a non-zero predator density equilibrium is stable (before crossing the Hopf bifurcation point) and the rodent biomass stabilizes at non-maximum values due to the predation pressure. After crossing a Hopf bifurcation, higher A values promoted the occurrence of stable orbits or limit cycles of increasing amplitude. The values of parameters C_1' and C_4' affected both the position of the Hopf bifurcation along the A-axis and the amplitude of the stable orbits. Higher values of C_4' restrict the stability of the fixed point to low values of A and promote larger amplitudes of limit cycles when they appear. Secondly, smaller values of C_1' exert an equivalent effect. Some trajectories of both state variables through time are shown in Fig. 6 for different values of A.

Hence, this analysis shows a destabilization effect of realized antipredator behavior on the non-trivial equilibrium point. This result contradicts the earlier paradigm of a stabilizing effect of refuge use in the context of simple models (Maynard-Smith, 1974; Murdoch and Oaten, 1975; Harrison, 1979; Ives and Dobson, 1987). Indeed, we performed further bifurcation analyses, setting the parameter to values at which the system exhibits a limit cycle when antipredator response is null. Increasing the response (parameter A) did not stabilize the equilibrium point in any case tested.

At this point, it will be useful to make clear our concept of antipredator effectiveness, which refers to the decrease in predation mortality rate as a consequence of the performance of some defensive trait by the prey. The exhibited defense makes the prey less likely to be detected, captured, or handled by the predator, which prevents its killing and consumption. In this sense, effectiveness of prey antipredator behavior is a synonym of the ineffectiveness of predators unless the prey response would prevent the consumption by the predator, but not the killing. In contrast, efficiency

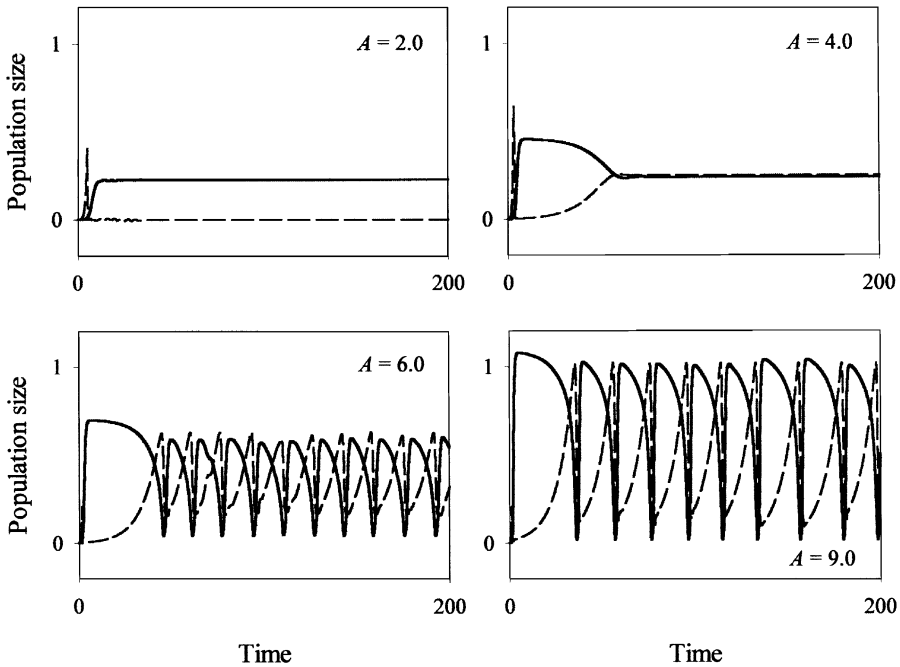

FIG. 6. Trajectories of state variables through time with four levels of antipredator effectiveness (A). Other parameter values as in Fig. 5(i): (continuous line) prey population; (dashed line) predator population.

measures (e.g., Ives and Dobson, 1987) must incorporate the different benefits and costs of the prey and predator performances. Hence, antipredator efficiency of prey could not be the same as predator inefficiency due to the particular trade-offs that influence each population.

Figure 7 shows bifurcation diagrams when foraging cost C_1' is the control parameter. The diagonal continuous straight line of negative slope indicates an equilibrium point, in which the predator equilibrium density is zero. Such a line is almost entirely composed by saddle points, shown as thin (unstable) lines. Other (non-straight) lines represent non-zero equilibrium densities for both prey and predators. An evaluation of the bifurcation diagrams shown in Fig. 7 shows both stabilizing and destabilizing effects when C_1' increases. Under high A and low C_4' values (Fig. 7(i)), the equilibrium is stable for low and intermediate levels of foraging cost. In such a region, the stable rodent equilibrium density decreases with larger values of C_1'. Under high levels of foraging cost the equilibrium is unstable and stable orbits appear, which in turn exhibit a decreasing amplitude as C_1' increases. A more complex situation appears in the neighborhood of the Hopf bifurcation, since three equilibrium points were found between $C_1' = 0.756$ and 0.764 (Fig. 8). Above the Hopf bifurcation (which is at $C_1' = 0.7637$), the upper and lower coexisting equilibrium points are unstable with both eigenvalues of the Jacobian matrix having positive real parts; and the middle one is a saddle. The upper point is stable below the Hopf bifurcation (Fig. 8). Furthermore, two limit cycles exist between $C_1' = 0.7631$ and the Hopf bifurcation, the wider being stable whereas the smaller being unstable (Fig. 7(i) and more clear in Fig. 8). Although not analytically proved, the numerical analysis indicates that this is a case of a subcritical Hopf bifurcation (Strogatz, 1994). In the region where the unstable orbit appears, this acts as a boundary between two domains of attraction, inside which all starting trajectories tend to the inner stable point. If trajectories start outside the unstable orbit, they reach a stable limit cycle. A similar result was obtained with the use of high values of parameter C_4' (Fig. 7(ii)), however, the amplitude of the stable limit cycle was larger, and stable limit cycles also appeared when the control parameter lies between $C_1' = 0.378$ and 0.569. Thus, conditions for stability are more restricted than in the previous case. Under intermediate values of A (Fig. 7(iii) and 7(iv)), the bifurcation diagrams show only one equilibrium point for any value of C_1'; in the case of low values of C_4' (Fig. 7(iii)) only one region of stable orbits was noticed. These cycles appear within a more restricted range of the control parameter (between $C_1' = 0.750$ and 0.848) where two supercritical Hopf

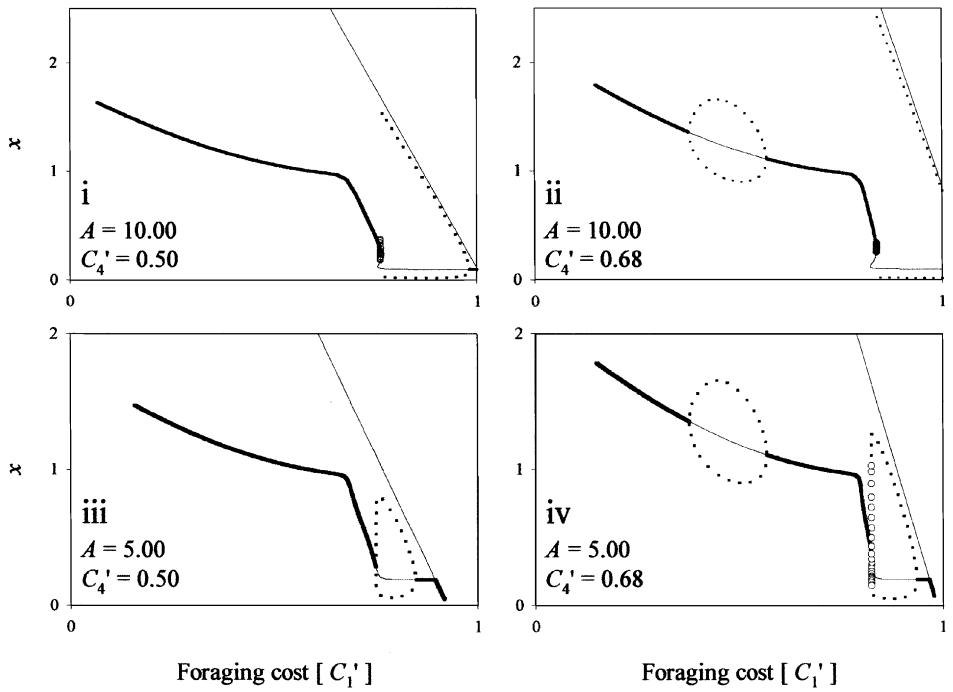

FIG. 7. Bifurcation diagrams when foraging cost is the control parameter. The values of A and C_4' are shown inside the graphs (horizontal arrows in Fig. 4): (thick line) stable fixed point; (thin continuous line) unstable fixed point; (dotted lines) maximum and minimum of stable orbits; (open circles) maximum and minimum of unstable orbits.

bifurcations occur. The last diagram (Fig. 7(iv)) shows one subcritical Hopf bifurcation at $C_1' = 0.8257$, below which an unstable orbit coexists with an outer, stable one. The second instability region was found between $C_1' = 0.378$ and 0.569, same as in Fig. 7(ii). A global evaluation of the bifurcation analyses summarized in Fig. 7 indicates that the equilibrium density of rodents decreases with increasing foraging costs. The equilibrium is mostly unstable under high values of C_1', but stable under low to intermediate C_1' values if C_4' is low; otherwise, we find a region of instability within a range of values of C_1'. Examples of prey and predator trajectories are shown in Fig. 9, illustrating the different possibilities just mentioned.

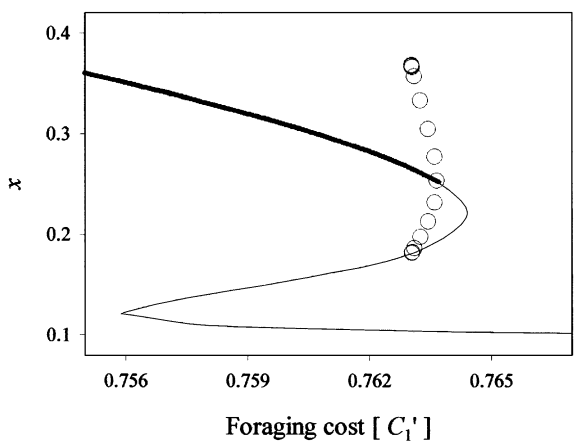

FIG. 8. A closer view of the region around the Hopf bifurcation of Fig. 6(i): (thick line) stable fixed point; (thin continuous line) unstable fixed point; (open circles) maximum and minimum of unstable orbits. Stable orbit not shown.

Bifurcation diagrams are shown in Fig. 10 when C_4', representing activity metabolism cost of antipredator behavior, is taken as the control parameter. As in the previous figures, the upper ("J" shaped) increasing lines in Fig. 10(i) and 10(iii) indicate zero equilibrium density of predators, where the unstable region of this line corresponds to saddle points. The first graph shows the behavior of equilibria; when low A and high C_1' values are used, and it reveals that a stable point exists for most of the tested values of C_4'. Below $C_4' = 0.583$, the model predicts a stable equilibrium density with zero density of predators (see trajectories in Fig. 11). The stable equilibrium is positive above that point for both populations and its values increase slowly with C_4'. Between $C_4' = 0.744$ and 0.760, we detected two stable points separated by one unstable (saddle) point at each C_4' value (see also Fig. 11). These bifurcation properties

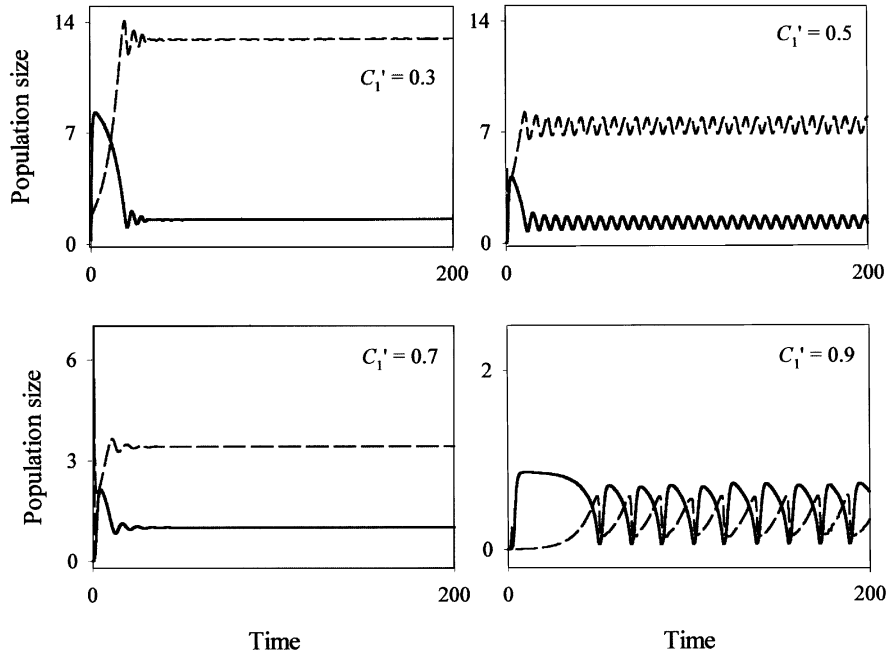

FIG. 9. Trajectories of state variables through time with four levels of foraging cost (C_1'). Other parameter values as in Fig. 7(iv): (continuous line) prey population; (dashed line) predator population.

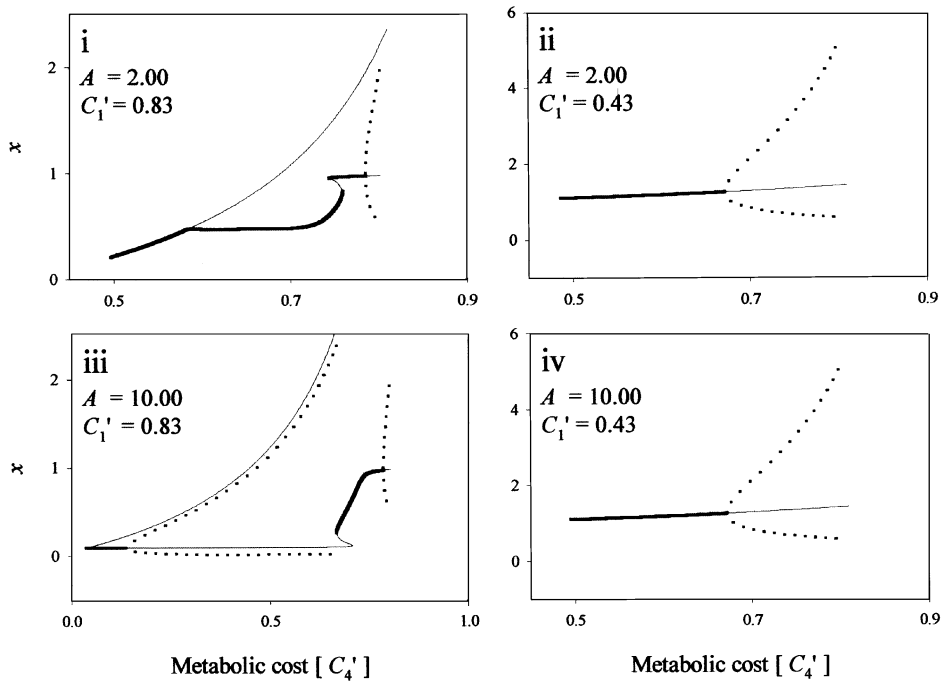

FIG. 10. Bifurcation diagrams when metabolic cost is the control parameter. The values of A of C_1' are shown inside the graphs (open diamonds in Fig. 4): (thick line) stable fixed point; (thin continuous line) unstable fixed point; (dotted lines) maximum and minimum of stable orbits.

determine an abrupt and non fully-reversible change in the equilibrium density of prey when the control parameter is varied, a phenomenon known as hysteresis. A supercritical hopf bifurcation point is found at $C_4' = 0.785$, above which a stable orbit with rapidly increasing amplitude appears (see the last graph of

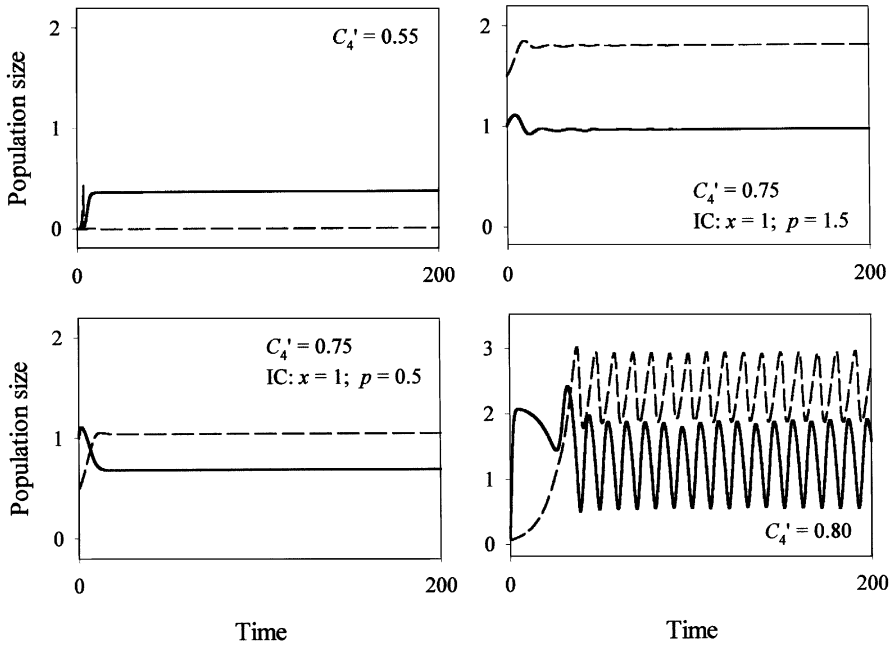

FIG. 11. Trajectories of state variables through time with four levels of metabolic cost (C_4'). Other parameter values as in Fig. 10(i): (continuous line) prey population; (dashed line) predator population. Upper-right and lower-left graphs show trajectories that started from different initial conditions (IC) and that converged toward each of the two stable equilibrium points (see Fig. 10).

Fig. 11). The equilibria are unstable under high values of A and for most C_4' values (Fig. 10(iii)). A first Hopf bifurcation is found at $C_4' = 0.136$ where stable limit cycles of exponentially increasing amplitude appear. When C_4' varies between 0.667 and 0.707 two unstable points and a stable one coexists, the last having a steeply increasing value as C_4' increases. The second supercritical Hopf bifurcation appeared at $C_4' = 0.785$, leading to a stable limit cycle. Figure 10(ii) and 10(iv) are identical, and show the bifurcation of equilibrium density of rodents when $C_1' = 0.433$, independent of the value of A. The zero predator density equilibria (not shown because of the scale of the graphs) were unstable (saddle) points, similar to that of Fig. 10(iii). Figure 10(ii) and 10(iv) show the existence of a unique stable point with C_4' values below the supercritical Hopf bifurcation at $C_4' = 0.671$, from which a stable orbit is found that reaches a large amplitude relative to the other analyzed cases.

The robustness of our results were corroborated by varying the values of parameters not considered in detail. We found no qualitative differences in the predictions when each parameter was perturbed up to 50% below and up to its referential value. The only differences detected corresponded to the precise position of the equilibrium and bifurcation points.

4. CONCLUSION

The analysis of our predator–prey model revealed that the relationship between stability of the non-trivial community equilibrium and reduced predation vulnerability, through refuge use by the prey, is strongly dependent upon the magnitude of the associated costs.

In particular, an increase in the metabolic cost of antipredator behavior promotes destabilization of the community equilibrium. The effect of increasing refuge use (i.e., decreasing vulnerability) may induce destabilization, depending on the values of other parameters. When no cost of activity metabolism and foraging exists, the equilibrium density of rodents remains stable independent of the antipredator behavior exhibited by the prey. If only a high foraging cost exists, the likelihood of instability increases with the effectiveness of antipredator response. When foraging cost is low or absent, the stability depends on the magnitude of the metabolic cost, but not on the antipredator effectiveness of prey. These patterns are graphically summarized in Fig. 12 with regard to the effect of increasing antipredator effectiveness, and under different combinations of cost magnitudes. Stability is sensitive to variations in antipredator effectiveness only when foraging cost is

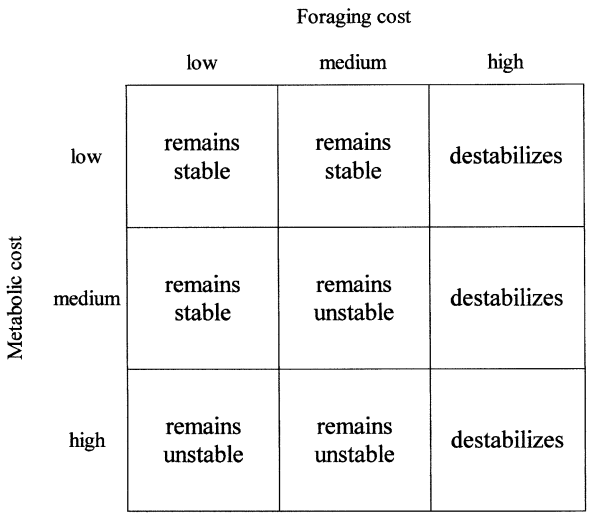

FIG. 12. Main effects of increasing antipredator effectiveness on the local stability of equilibrium points. The different scenarios are combinations of low/medium/high levels of foraging and metabolic costs.

high. On the other hand, if we consider only low to medium foraging costs, the equilibria are stable when both costs are low, but unstable when both costs are higher, independent of antipredator effectiveness. No evidence of stabilizing effects of antipredator behavior was found in the context of our approach.

Therefore, our analysis suggests that the trade-offs involved in antipredator behavior play a fundamental role in the stability properties of the system. The gross growth rate is lower and metabolic losses are higher when costs are high, which results in slower population growth. This implies that the impact of predation is stronger and dominates the system dynamics, and promotes population oscillations (Berryman, 1999). In a future paper, we will test these predictions by using simpler population models with alternative structures but retaining empirically founded cost–benefit relationships.

In this study, we have constructed a non-structured population model incorporating behavioral and eco-physiological information of the leaf-eared mouse *P. darwini*. We have shown that the stability properties of the system include, for certain parameter ranges, stable and unstable points as well as stable and unstable limit cycles. Regarding the population outbreaks exhibited in the field by *P. darwini* (Lima *et al.*, 1999a), our model shows both large-amplitude stable cycles and multiple stable equilibrium points, which are the most accepted alternative dynamical properties that explain the occurrence of outbreaks (Berryman, 1990).

Given the wide range of potential dynamics allowed by this model, a useful progress would be to restrict the parameter space to those values that maximize the per capita growth rate of prey. Although such an optimality approach (e.g., Ives and Dobson 1987) imposes restrictive assumptions that do not necessarily hold true for natural populations, it would be insightful to compare the dynamic outcomes of adaptive versus non-adaptive behavior.

Finally, the quantitative aspects of the model predictions need to be more accurately assessed using other tools if a greater correspondence between model and nature is needed.

APPENDIX A

The proposed model obeys

$$\frac{dX}{dt} = X[G - M - D], \tag{A1}$$

$$\frac{dP}{dt} = f(H(X,P))P. \tag{A2}$$

In which the rate of gross growth of rodents is given by the function $G(X)$, expressed as

$$G(X) = \frac{gR^{\lambda}\xi_A\xi_C}{\beta^{\lambda} + (\gamma X)^{\lambda} + R^{\lambda}} \tag{A3}$$

noting that

$$\lim_{R\to\infty} G(X) = \lim_{R\to\infty}\left(\frac{g\xi_A\xi_C}{(\beta/R)^{\lambda} + (\gamma X/R)^{\lambda} + 1}\right) = g\xi_A\xi_C.$$

and metabolic losses are defined as

$$M(P) = \mu_R + \mu_A = \mu_R + \omega(\mu_M - \mu_R). \tag{A4}$$

The antipredator response is assumed to be a function of predator density in the form:

$$V(P) = \frac{1 - V_\alpha}{1 + (P/P_u)^z} + V_\alpha \tag{A5}$$

and substituting $p = P/P_u$, we obtain the relation

$$V(p) = \frac{1 - V_\alpha + V_\alpha(1 + p^z)}{1 + p^z} = \frac{1 + V_\alpha p^z}{1 + p^z}. \tag{A6}$$

The trade-offs between vulnerability to predators and, metabolism and foraging, respectively, are given by

$$\omega(V) = \frac{V(\omega_\infty - \omega_0)}{V_\omega + V} + \omega_0, \tag{A7}$$

$$g(V) = \frac{V(g_\infty - g_0)}{V_g + V} + g_0. \tag{A8}$$

By substituting function (A6) into (A8), we obtain

$$g(p) = \frac{(g_\infty - g_0)(1 + p^z V_\alpha)}{1 + V_g + p^z(V_g + V_\alpha)} + g_0 \tag{A9}$$

factorizing by V_α and by $V_g + V_\alpha$, the above equations become either

$$g(p) = \frac{V_\alpha(g_\infty - g_0)(1/V_\alpha + p^z)}{(V_g + V_\alpha)((1 + V_g)/(V_g + V_\alpha) + p^z)} + g_0 \tag{A10}$$

or

$$g(p) = \frac{V_\alpha(g_\infty - g_0)}{V_g + V_\alpha}\left(\frac{1/V_\alpha + p^z}{(1 + V_g)/(V_g + V_\alpha) + p^z} + \frac{(V_g + V_\alpha)g_0}{V_\alpha(g_\infty - g_0)}\right). \tag{A11}$$

Likewise, by substituting (A6) into (A7) and then factorizing, we obtain

$$\omega(p) = \frac{V_\alpha(\omega_\infty - \omega_0)}{V_\omega + V_\alpha}\left(\frac{1/V_\alpha + p^z}{(1 + V_\omega)/(V_\omega + V_\alpha) + p^z} + \frac{(V_\omega + V_\alpha)\omega_0}{V_\alpha(\omega_\infty - \omega_0)}\right). \tag{A12}$$

According to Eq. (11) (see text), the per capita gross growth rate of rodents is

$$G(X, P) = \frac{R^\lambda \xi_A \xi_C}{\beta^\lambda + (\gamma X)^\lambda + R^\lambda} \times \left[\frac{(g_\infty - g_0)(P_u^z + P^z V_\alpha)}{P_u^z(V_g + 1) + P^z(V_g + V_\alpha)} + g_0\right]. \tag{A13}$$

Substituting (A11) into (A13) yields

$$G(X, p) = \frac{V_\alpha(g_\infty - g_0)}{V_g + V_\alpha}\left(\frac{1/V_\alpha + p^z}{(1 + V_g)/(V_g + V_\alpha) + p^z} + \frac{(V_g + V_\alpha)g_0}{V_\alpha(g_\infty - g_0)}\right) \times \frac{R^\lambda \xi_A \xi_C}{\beta^\lambda + (\gamma X)^\lambda + R^\lambda}. \tag{A14}$$

Likewise, the metabolism function $M(P)$ defined in Eq. (12) (see text) can be set in a similar way to yield

$$M(p) = \mu_R + \left(\frac{(\omega_\infty - \omega_0)(1 + p^z V_\alpha)}{1 + V_\omega + p^z(V_\omega + V_\alpha)} + \omega_0\right) \times (\mu_M - \mu_R) \tag{A15}$$

and

$$M(p) = \mu_R + \frac{V_\alpha(\omega_\infty - \omega_0)}{V_\omega + V_\alpha} \times \left(\frac{1/V_\alpha + p^z}{(1 + V_\omega)/(V_\omega + V_\alpha) + p^z} + \frac{(V_\omega + V_\alpha)\omega_0}{V_\alpha(\omega_\infty - \omega_0)}\right) \times (\mu_M - \mu_R). \tag{A16}$$

The mortality function (Eq. (10)) expressed in terms of p yields

$$D(X, p) = \frac{pP_u\phi}{X}\left[1 + \left(\frac{1 + p^z}{X(1 + V_\alpha p^z)}\right)^\Lambda \times (\tau^\Lambda + (\Gamma P_u p)^\Lambda)\right]^{-1}. \tag{A17}$$

In order to reduce the number of parameters, we define

$$E_1 = \frac{V_\alpha(g_\infty - g_0)}{V_g + V_\alpha} R^\lambda \xi_A \xi_C, \tag{A18}$$

$$N = \beta^\lambda + R^\lambda, \tag{A19}$$

$$A = \frac{1}{V_\alpha}, \tag{A20}$$

$$B_1 = \frac{V_g + 1}{V_g + V_\alpha}, \tag{A21}$$

$$C_1 = \frac{g_0(V_g + V_\alpha)}{V_\alpha(g_\infty - g_0)} \tag{A22}$$

to obtain

$$G(X, p) = \left(\frac{A + p^z}{B_1 + p^z} + C_1\right)\frac{E_1}{N + (\gamma X)^\lambda}. \tag{A23}$$

Likewise, we reduced the number of parameters in the metabolic function obtaining

$$M(p) = \mu_R + E_2\left(\frac{A + p^z}{B_2 + p^z} + C_2\right)(\mu_M - \mu_R), \tag{A24}$$

where

$$C_2 = \frac{\omega_0(V_\omega + V_\alpha)}{V_\alpha(\omega_\infty - \omega_0)}, \tag{A25}$$

$$E_2 = \frac{V_\alpha(\omega_\infty - \omega_0)}{V_\omega + V_\alpha}, \tag{A26}$$

$$B_2 = \frac{V_\omega + 1}{V_\omega + V_\alpha}. \tag{A27}$$

Furthermore, Eq. (A24) can be written as

$$M(p) = E_2(\mu_M - \mu_R) \times \left(\frac{\mu_R}{E_2(\mu_M - \mu_R)} + \frac{A + p^z}{B_2 + p^z} + C_2\right), \tag{A28}$$

$$M(p) = C_3\left(\frac{A + p^z}{B_2 + p^z} + C_4\right), \tag{A29}$$

where

$$C_3 = E_2(\mu_M - \mu_R), \tag{A30}$$

$$C_4 = \frac{\mu_R}{E_2(\mu_M - \mu_R)} + C_2. \tag{A31}$$

The mortality function of prey (Eq. (A17)), can be written as

$$D(X, p) = \frac{pP_u\phi}{X}\left[1 + \left(\frac{\Gamma P_u}{V_\alpha}\right)^\Lambda \left(\frac{1 + p^z}{X(1/V_\alpha + p^z)}\right)^\Lambda \times \left(\left(\frac{\tau}{\Gamma P_u}\right)^\Lambda + p^\Lambda\right)\right] \tag{A32}$$

or

$$D(X, p) = \frac{pP_u\phi}{X} \times \left[1 + K_1\left(\frac{1 + p^z}{X(A + p^z)}\right)^\Lambda (K_2 + p^\Lambda)\right], \tag{A33}$$

where

$$K_1 = \left(\frac{\Gamma P_u}{V_\alpha}\right)^\Lambda, \tag{A34}$$

$$K_2 = \left(\frac{\tau}{\Gamma P_u}\right)^\Lambda. \tag{A35}$$

The above steps lead to the following equation for the prey population:

$$\frac{dX}{dt} = X\left[\left(\frac{A + p^z}{B_1 + p^z} + C_1\right)\frac{E_1}{N + (\gamma X)^\lambda} - C_3\left(\frac{A + p^z}{B_2 + p^z} + C_4\right) - \frac{pP_u\phi}{X} \times \left[1 + K_1\left(\frac{1 + p^z}{X(A + p^z)}\right)^\Lambda (K_2 + p^\Lambda)\right]^{-1}\right]. \tag{A36}$$

If we redefine the state-variable $X = N^{1/\lambda}x/\gamma$ and $dX/dt = N^{1/\lambda}/\gamma\, dx/dt$, we obtain

$$\frac{dx}{dt} = x\frac{E_1}{N}\left[\left(\frac{A + p^z}{B_1 + p^z} + C_1\right)\frac{1}{1 + x^\lambda} - C_3\frac{N}{E_1}\left(\frac{A + p^z}{B_2 + p^z} + C_4\right) - \frac{N}{E_1}\frac{pP_u\phi\gamma}{N^{1/\lambda}x} \times \left[1 + K_1\left(\frac{\gamma(1 + p^z)}{N^{1/\lambda}x(A + p^z)}\right)^\Lambda (K_2 + p^\Lambda)\right]^{-1}\right], \tag{A37}$$

$$\frac{dx}{dt} = xE\left[\left(\frac{A + p^z}{B_1 + p^z} + C_1\right)\frac{1}{1 + x^\lambda} - C_5\left(\frac{A + p^z}{B_2 + p^z} + C_4\right) - \frac{C_7 p}{x} \times \left[1 + C_6\left(\frac{1 + p^z}{x(A + p^z)}\right)^\Lambda (K_2 + p^\Lambda)\right]^{-1}\right] \tag{A38}$$

in which

$$E = \frac{E_1}{N}, \tag{A39}$$

$$C_5 = C_3\frac{N}{E_1}, \tag{A40}$$

$$C_6 = \frac{K_1\gamma^\Lambda}{N^{\Lambda/\lambda}}, \tag{A41}$$

$$C_7 = \frac{N}{E_1}\frac{P_u\phi\gamma}{N^{1/\lambda}}. \tag{A42}$$

If the parameter and variable definitions given above are considered, the predator equation given in the text as

$$\frac{dP}{dt} = P\rho\left[1 - \frac{\kappa P}{XD(X, P)}\right] \tag{A43}$$

can be written as follows:

$$\frac{dp}{dt} = p\rho\left[1 - \frac{\kappa}{\phi} \times \left(1 + C_6\left(\frac{1 + p^z}{x(A + p^z)}\right)^\Lambda (K_2 + p^\Lambda)\right)\right]. \tag{A44}$$

Thus,

$$\frac{dp}{dt} = p\rho\frac{\phi - \kappa}{\phi} \times \left[1 - \frac{\kappa}{\phi - \kappa}C_6\left(\frac{1 + p^z}{x(A + p^z)}\right)^\Lambda (K_2 + p^\Lambda)\right], \tag{A45}$$

$$\frac{dp}{dt} = pK_4\left[1 - K_5\left(\frac{1+p^z}{x(A+p^z)}\right)^{\Lambda}(K_2+p^{\Lambda})\right], \quad \text{(A46)}$$

where

$$K_4 = \rho\frac{\phi-\kappa}{\phi}, \quad \text{(A47)}$$

$$K_5 = \frac{\kappa}{\phi-\kappa}C_6. \quad \text{(A48)}$$

By combining the prey and predator equations, we obtain the system

$$\frac{dx}{dt} = xE\Bigg[\left(\frac{A+p^z}{B_1+p^z}+C_1\right)\frac{1}{1+x^{\lambda}} - C_5\left(\frac{A+p^z}{B_2+p^z}+C_4\right) - \frac{C_7 p}{x} \times\left[1+C_6\left(\frac{1+p^z}{x(A+p^z)}\right)^{\Lambda}(K_2+p^{\Lambda})\right]^{-1}\Bigg], \quad \text{(A49)}$$

$$\frac{dp}{dt} = pK_4\left[1 - K_5\left(\frac{1+p^z}{x(A+p^z)}\right)^{\Lambda}(K_2+p^{\Lambda})\right]. \quad \text{(A50)}$$

Finally, setting

$$C_9 = \frac{K_4}{E} \quad \text{(A51)}$$

and rescaling the time as $\mathrm{T} = Et$ and thus $dx/dt = dx/d\mathrm{T}\,d\mathrm{T}/dt$ and $dp/dt = dp/d\mathrm{T}\,d\mathrm{T}/dt$ we obtain the 14-parameter system:

$$\frac{dx}{d\mathrm{T}} = x \times\Bigg[\left(\frac{A+p^z}{B_1+p^z}+C_1\right)\frac{1}{1+x^{\lambda}} - C_5\left(\frac{A+p^z}{B_2+p^z}+C_4\right) - \frac{C_7 p}{x}\left[1+C_6\left(\frac{1+p^z}{x(A+p^z)}\right)^{\Lambda}(K_2+p^{\Lambda})\right]^{-1}\Bigg], \quad \text{(A52)}$$

$$\frac{dp}{d\mathrm{T}} = pC_9 \times\left[1 - K_5\left(\frac{1+p^z}{x(A+p^z)}\right)^{\Lambda}(K_2+p^{\Lambda})\right]. \quad \text{(A53)}$$

ACKNOWLEDGMENTS

This work was supported by FONDECYT grants 3000051 to R.R.J., 1010399 to E.G.O., and 1010950 to F.B. We sincerely thank W.M. Getz, P.A. Marquet, M. Lima, and two anonymous reviewers for their valuable suggestions. We also thank G.B. Ermentrout for technical help with XPPAUT, and L.A. Ebensperger for English corrections.

REFERENCES

Abrams, P. A., and Walters, C. J. 1996. Invulnerable prey and the paradox of enrichment, *Ecology* **77**, 1125–1133.

Beddington, J. R. 1975. Mutual interference between parasites or predators and its effect on searching efficiency, *J. Anim. Ecol.* **44**, 331–340.

Berryman, A. A. 1990. Identification of outbreak classes, *Math. Comput. Model.* **13**, 105–116.

Berryman, A. A. 1992. The origins and evolution of predator–prey theory, *Ecology* **73**, 1530–1535.

Berryman, A.A. 1999. "Principles of Population Dynamics and their Application", Stanley Thornes Ltd., Cheltenham, U.K.

Bozinovic, F. 1997. Diet selection in rodents: an experimental test of the effect of dietary fiber and tannins on feeding behavior, *Rev. Chil. Hist. Nat.* **70**, 67–71.

Bozinovic, F., and Merritt, J. F. 1991. Conducta, estructura y función de micromamíferos en ambientes estacionales: mecanismos compensatorios, *Rev. Chil. Hist. Nat.* **64**, 19–28.

Bozinovic, F., and Nespolo, R. F. 1997. Effect of ambient temperature and energy demands on digestive functions in leaf-eared mice (*Phyllotis darwini*) From central Chile, *Int. J. Biometeorol.* **41**, 23–25.

Bozinovic, F., and Novoa, F. F. 1997. Metabolic costs of rodents feeding on plant chemical defenses: a comparison between an herbivore and an omnivore, *Comp. Biochem. Physiol.* **117A**, 511–514.

Bozinovic, F., and Rosenmann, M. 1988. Comparative energetics of South American cricetid rodents, *Comp. Biochem. Physiol.* **91A**, 195–202.

Bozinovic, F., and Rosenmann, M. 1989. Maximum metabolic rate of rodents: physiological and ecological consequences on distributional limits, *Funct. Ecol.* **3**, 173–181.

Bozinovic, F., Novoa, F. F., and Nespolo, R. F. 1997. Effect of dietary composition on food selection and assimilation in the leaf-eared mouse (*Phyllotis darwini*) inhabiting central Chile, *Rev. Chil. Hist. Nat.* **70**, 289–295.

Bozinovic, F., Rosenmann, M., and Veloso, C. 1988. Termorregulación conductual en *Phyllotis darwini* (Rodentia: Cricetidae): efecto de la temperatura ambiente, uso de nidos y agrupamiento social sobre el gasto de energía, *Rev. Chil. Hist. Nat.* **61**, 81–86.

Canals, M., Rosenmann, M., and Bozinovic, F. 1997. Geometrical aspects of the energetic effectiveness of huddling in small mammals, *Acta Theriol.* **42**, 321–328.

DeAngelis, D. L., Goldstein, R. A., and O'Neill, R. V. 1975. A model for trophic interaction, *Ecology* **56**, 881–892.

Ebensperger, L. A. 1996. The fasting endurance hypothesis: the case of two rodent species from central Chile, *Rev. Chil. Hist. Nat.* **69**, 57–65.

Ermentrout, G. B. 2000. "XPPAUT 4.0: the differential equations tool" Available at: http://www.math.pitt.edu/~bard/xpp/xpp.html.

Getz, W. M. 1984. Population dynamics: a resource per capita approach, *J. Theor. Biol.* **108**, 623–644.

Getz, W. M. 1991. A unified approach to multispecies modeling, *Nat. Resour. Model.* **5**, 393–421.

Getz, W. M. 1993. Metaphysiological and evolutionary dynamics of populations exploiting constant and interactive resources: r–K selection revisited, *Evolutionary Ecol.* **7**, 287–305.

Getz, W. M. 1994. A metaphysiological approach to modeling ecological populations and communities, *in* "Frontiers in Mathematical Biology" (S. A. Levin, Ed.), Lecture Notes in Biomathematics, Vol. 100, pp. 411–442, Springer-Verlag, New York.

Ginzburg, L. R. 1998. Assuming reproduction to be a function of consumption raises doubts about some popular predator–prey models, *J. Anim. Ecol.* **67**, 325–327.

Gorecki, A. 1965. Energy values of body in small mammals, *Acta Theriol.* **10**, 333–352.

Grodzinski, W., and Wunder, B.A. 1975. Ecological energetics of small mammals, *in* "Small Mammals: Their Productivity and Population Dynamics" (F. B. Golley, K. Petrusewicz, and L. Ryszkowsky, Eds.), pp. 173–204, Cambridge University Press, Cambridge.

Harrison, G. W. 1979. Global stability of predator–prey interactions, *J. Math. Biol.* **8**, 159–171.

Harvell, C. D., and Tollrian, R. 1999. Why inducible defenses?, *in* "The Ecology and Evolution of Inducible Defenses" (R. Tollrain and C. D. Harvell, Eds.), pp. 3–9, Princeton University Press, Princeton, NJ.

Holling, C. S. 1959. The components of predation as revealed by a study of small mammal predation of the European pine sawfly, *Can. Entomol.* **91**, 293–320.

Ives, A.R., and Dobson, A.P. 1987. Antipredator behavior and the population dynamics of simple predator–prey systems, *Am. Nat.* **130**, 431–447.

Jaksic, F. M. 1997. "Ecología de los vertebrados de Chile", Ediciones Universidad Católica de Chile, Santiago.

Jimenez, J. E., Feinsinger, P., and Jaksic, F. M. 1992. Spatiotemporal patterns of an irruption and decline of small mammals on north central Chile, *J. Mammal.* **73**, 356–364.

Kauffman, D. W., Kaufman, G. A., and Wiener, J. G. 1975. Energy equivalents for sixteen species of xeric rodents, *J. Mammal.* **56**, 946–949.

Křivan, V. 1998. Effects of optimal antipredator behavior of prey on predator–prey dynamics: the role of refuges, *Theor. Popul. Biol.* **53**, 131–142.

Leslie, P. H. 1948. Some further notes on the use of matrices in population mathematics, *Biometrika* **35**, 213–245.

Lima, M., and Jaksic, F. M. 1998a. Delayed density-dependence and rainfall effects on reproductive parameters of an irruptive rodent in semiarid Chile, *Acta Theriol.* **43**, 225–236.

Lima, M., and Jaksic, F. M. 1998b. Population variability among three small mammal species in the semiarid Neotropics: the role of density-dependent and density-independent factors, *Ecography* **21**, 175–180.

Lima, M., and Jaksic, F. M. 1999a. Population dynamics of three Neotropical small mammals: time series models and the role of delayed density-dependence in population irruptions, *Aust. J. Ecol.* **24**, 25–34.

Lima, M., and Jaksic, F. M. 1999b. Population rate of change in the leaf-eared mouse: the role of density-dependence, seasonality and rainfall, *Aust. J. Ecol.* **24**, 110–116.

Lima, M., Keymer, J. E., and Jaksic, F. M. 1999a. ENSO-driven rainfall variability and delayed density-dependence cause rodent outbreaks in western South America: linking demography and population dynamics, *Am. Nat.* **153**(5), 476–491.

Lima, M., Marquet, P. A., and Jaksic, F. M. 1999b. EI Niño events, precipitation patterns, and rodent outbreaks are statistically associated in semiarid Chile, *Ecography* **22**, 213–218.

Lima, M., Julliard, R., Stenseth, N. C., and Jaksic, F. M. 2001. Demographic dynamics of a Neotropical small rodent (*Phyllotis darwini*): feedback structures, predation and climate. *J. Anim Ecol.* **70**, 761–775.

Maynard-Smith, J. 1974. "Models in ecology." Cambridge University Press, Cambridge.

McNair, J. 1986. The effects of refuges on predator–prey interactions: a reconsideration. *Theor. Popul. Biol.* **29**, 38–63.

Meserve, P. L. 1981. Trophic relationships among small mammals in a Chilean semiarid thorn scrub community, *J. Mammal.* **62**, 304–314.

Meserve, P. L., Gutiérrez, J. R., Yunger, J. A., Contreras, L. C., and Jaksic, F. M. 1996. Role of biotic interactions in a small mammal assemblage in semiarid Chile, *Ecology* **77**, 133–148.

Meserve, P. L., and LeBoulengé, E. 1987. Population dynamics and ecology of small mammals in the northern Chilean semiarid region. Studies in Neotropical Mammalogy, *Fieldiana, Zool. New Series* **39**, 413–431.

Murdoch, W. W., and Oaten, A. 1975. Predation and population stability, *Adv. Ecol. Res.* **9**, 1–131.

Pitts, D. R., and Sissom, L. E. 1979. "Teoría y problemas de transferencia de calor." McGraw-Hil Latinoamericana, S.A., Bogotá.

Ruxton, G. D. 1995. Short term refuge use and stability of predator–prey models, *Theor. Popul. Biol.* **47**, 1–17.

Sih, A. 1987a. Prey refuges and predator–prey stabillity, *Theor. Popul. Biol.* **31**, 1–12.

Sih, A. 1987b. Predators and prey lifestyles: an evolutionary and ecological overview, *in* "Predation. Direct and Indirect Impacts on Aquatic Communities" (W. C. Kerfoot and A. Sih, Eds.), pp. 203–224, University Press of New England, Hanover, NH.

Sih, A., Petranka, J. W., and Kats, L. B., 1988. The dynamics of prey refuge use: a model and tests with sunfish and salamander larvae, *Am. Nat.* **132**, 463–483.

Simonetti, J. A. 1989. Microhabitat use by small mammals in central Chile, *Oikos* **56**, 309–318.

Strogatz, S. H. 1994. "Nonlinear Dynamics and Chaos. With Applications to Physics, Biology, Chemistry, and Engineering," Peresus Publishing, Cambridge, Massachusetts.

Tollrian, R., and Harvell, C. D., 1999. "The Ecology and Evolution of Inducible Defenses," Princeton University Press, Princeton, NJ.

Vásquez, R. A., 1994. Assessment of predation risk via illumination level: facultative central place foraging in the cricetid rodent *Phyllotis darwini*, *Behav. Ecol. Sociobiol.* **34**, 375–381.

Vásquez, R. A. 1996. Patch utilization by three species of Chilean rodents differing in body size and mode of locomotion, *Ecology* **77**, 2343–2351.

Wunder, B. A. 1978. Implication of a conceptual model for the allocation of energy resources by small mammals, *in* "Populations of Small Mammals under Natural Conditions. Pymatuning Laboratory of Ecology" (O. Snyder, Ed.), pp. 68–75, University of Pittsburgh Special Publication Series 5, Pittsburgh, PA.